RING FORMATION IN MAGNETICALLY SUBCRITICAL CLOUDS AND MULTIPLE STAR FORMATION

Zhi-Yun Li
Department of Astronomy, University of Virginia, P.O. Box 3818
Charlottesville, VA 22903; zl4h@virginia.edu

ABSTRACT

We study numerically the ambipolar diffusion-driven evolution of non-rotating, magnetically subcritical, disk-like molecular clouds, assuming axisymmetry. Previous similar studies have concentrated on the formation of single magnetically supercritical cores at the cloud center, which collapse to form isolated stars. We show that, for a cloud with many Jeans masses and a relatively flat mass distribution near the center, a magnetically supercritical ring is produced instead. The supercritical ring contains a mass well above the Jeans limit. It is expected to break up, through both gravitational and possibly magnetic interchange instabilities, into a number of supercritical dense cores, whose dynamic collapse may give rise to a burst of star formation. Non-axisymmetric calculations are needed to follow in detail the expected ring fragmentation into multiple cores and the subsequent core evolution. Implications of our results on multiple star formation in general and the northwestern cluster of protostars in the Serpens molecular cloud core in particular are discussed.

Subject headings: ISM: clouds — ISM: magnetic fields — MHD — stars: formation

1. INTRODUCTION

At the heart of multiple star formation lies cloud fragmentation. The role of magnetic fields in the cloud fragmentation is not well explored (Boss 2001), even though present day molecular clouds are thought to be strongly magnetized. Reliable Zeeman measurements of the magnetic field strength of molecular clouds made to date, as compiled by Crutcher (1999), suggest that, after geometric corrections (Shu et al. 1999), the clouds are remarkably close to being magnetically critical. These measurements reinforce the oft-expressed view that magnetic fields in molecular clouds are strong enough to be dynamically important.

Dynamically important magnetic fields can change the characteristics of cloud fragmentation fundamentally. The magnetic and gravitational forces are often comparable in magnitude but opposite in direction. The near cancellation of forces (Shu & Li 1997) can in principle keep the clouds in a magnetically levitated state over many dynamic times, allowing more time for over dense substructures to develop and fragment. To isolate the effects of magnetic fields on cloud fragmentation from those of turbulence (which have been the subject of intensive numerical simulations, as reviewed by Vazquez-Semadeni et al. 2000), we will concentrate on the relatively quiescent regions of molecular clouds. Such regions are capable of producing binaries, multiple stellar systems, as well as groups or small clusters - all of which we broadly term "multiple stars" - but not rich clusters of hundreds to thousands of stars, which tend to form in more turbulent regions (Myers 1999). Our goal is to extend the reasonably successful scenario of single, isolated star formation, based on ambipolar diffusion (Shu, Adams & Lizano 1987; Mouschovias & Ciolek 1999; see, however, Nakano 1998 for a different opinion), to the formation of multiple stars. In a longer term, we hope to apply the insight gained on the magnetically controlled fragmentation and multiple star formation to the more difficult problem of rich cluster formation, where turbulence plays a more dominant role (e.g., Klessen, Burkert & Bate 1998).

In the absence of a strong turbulence, a cloud with many Jeans masses supported mainly by an ordered magnetic field tends to settle along field lines into a disk-like configuration (Mouschovias 1976; Tomisaka, Ikeuchi & Nakamura 1988). The flattened geometry promotes cloud fragmentation which, under strict axisymmetry, manifests itself in the formation of *gravitationally unstable rings*, even in the absence of any rotation. This was demonstrated explicitly by Bastien (1983) for non-magnetic clouds. Physically, the ring formation results from the fact that it would take less time for a Jeans mass of material located more than one Jeans length from the cloud center to collapse freely onto itself than to reach the center. The reason is simply that free fall time is inversely proportional to the square root of (average) density. For a more or less uniform mass distribution, the local density at the off-center location is higher than the average density interior to it, since

most of the interior is empty for a flattened structure (Bonnell 1999). In this paper, we will demonstrate that strong magnetic fields do not fundamentally alter the natural tendency of *flattened* multi-Jeans mass clouds to form rings in the axisymmetric geometry, even though the fields provide the bulk of cloud support, flatten the cloud material (thus making ring formation possible in the first place), and control the pace of cloud evolution (through ambipolar diffusion). This behavior is consistent with the linear analysis of Langer (1978; see also Pudritz 1990), who considered the Jeans instability in an infinite, lightly ionized, isothermal medium with a uniform density and magnetic field. Employing the standard "Jeans swindle", Langer was able to show that the presence of a magnetic field does not change the critical wavelength (and thus mass) above which the instability occurs, although the growth rate can be strongly modified: for typical dark cloud conditions the instability grows on an ambipolar diffusion time scale, which is roughly an order of magnitude longer than the dynamic time scale. One expects the same magnetically-retarded Jeans instability to operate in the magnetically supported, disk-like clouds of finite extent as well. Indeed, our calculations of ring formation in such clouds can be viewed as following the nonlinear developments of the instability under the restriction of axisymmetry.

Dense rings sometimes appear in numerical simulations of axisymmetric collapse of *non-magnetic, rotating* clouds (e.g., Black & Bodenheimer 1976). They are shown to be strongly susceptible to dynamical non-axisymmetric fragmentation into small pieces (Norman & Wilson 1980). These rotating rings were widely discussed in connection with the production of multiple stellar systems in late 1970s and early 1980s, although their formation depends sensitively on the numerical treatment of angular momentum transport (Norman, Wilson & Barton 1980). The ring formation to be discussed in this paper does not depend on rotation. It represents a first step towards a theory of multiple star formation in a strongly magnetized cloud.

The rest of the paper is organized as follows. The mathematical formulation of the problem of ring formation in a strongly magnetized cloud is given in § 2, and numerical examples are presented in § 3. We discuss in § 4 ring fragmentation and its implications on multiple star formation in general and the northwestern cluster of the Serpens molecular cloud core in particular.

2. FORMULATION OF THE PROBLEM

2.1. Governing Equations

We adopt the standard thin-disk approximation (e.g., Nakamura, Hanawa & Nakano 1995) and cast the MHD equations that govern the evolution of magnetized clouds in a vertically integrated form. Mass conservation of the disk material yields

$$\frac{\partial \Sigma}{\partial t} + \frac{1}{r}\frac{\partial}{\partial r}(r\Sigma V) = 0, \tag{1}$$

where Σ, t, r, and V are, respectively, the (mass) column density, time, cylindrical radius, and the radial component of disk velocity. Axisymmetry and a cylindrical coordinate system (r, ϕ, z) are adopted throughout the paper.

We assume that the disk is isothermal with an effective sound speed of a and is threaded by an ordered magnetic field with a (cylindrically) radial component B_r and a vertical component B_z. The vertically integrated momentum equation in the radial direction then becomes

$$\frac{\partial (\Sigma V)}{\partial t} + \frac{1}{r}\frac{\partial}{\partial r}(r\Sigma V^2) = \Sigma g_r + \frac{B_r B_z}{2\pi} - \frac{\partial (\Sigma a^2)}{\partial r} - H\frac{\partial}{\partial r}\left(\frac{B_z^2}{4\pi}\right), \tag{2}$$

where g_r is the radial component of gravity and H is the disk half thickness. The force terms on the right-hand side of the equation are, respectively, gravity, magnetic tension, thermal (and possibly turbulent) and magnetic pressure force. We have kept only the leading terms for the magnetic tension and pressure force, and have ignored cloud rotation, which is dynamically unimportant in general before the formation of compact stellar objects (i.e., protostars and their disks; see Basu & Mouschovias 1994). Rotation can easily be included if necessary.

The evolution of the ordered magnetic field is governed by the magnetic flux conservation equation

$$\frac{\partial B_z}{\partial t} + \frac{1}{r}\frac{\partial}{\partial r}(r B_z V_{_B}) = 0, \tag{3}$$

where $V_{_B}$ is the velocity of magnetic field lines in the cross-field direction (Nakano 1984). In a lightly ionized medium such as molecular cloud, the field lines slip relative to the neutral matter at a velocity

$$V_{_B} - V = t_c \left[\frac{B_r B_z}{2\pi} - H\frac{\partial}{\partial r}\left(\frac{B_z^2}{4\pi}\right)\right] \Big/ \Sigma, \tag{4}$$

where t_c is the coupling time between the magnetic field and neutral matter. In the simplest case where the coupling is provided by ions that are well tied to the field lines and the ion density ρ_i is related to the cloud density ρ by the simple expression $\rho_i = C\rho^{1/2}$, one has

$$t_c = \frac{1.4}{\gamma C \rho^{1/2}}, \tag{5}$$

where typically $\gamma C = 1.05 \times 10^{-2} \mathrm{cm}^{3/2} \mathrm{g}^{-1/2}\ \mathrm{s}^{-1}$ (e.g., Shu 1992) and the factor 1.4 comes from the fact that the cross section for ion-helium collision is small compared to that of ion-hydrogen collision (Mouschovias & Morton 1991).

The disk half thickness H in equation (2) and the mass density ρ in equation (5) are related through the definition

$$\Sigma = 2\rho H. \tag{6}$$

To determine these two quantities separately, we assume that the disk is always in a static equilibrium in the disk-normal direction (Fiedler & Mouschovias 1993). Integration of the force balance equation vertically yields

$$\rho = \frac{\pi G \Sigma^2}{2a^2} \left(1 + \frac{B_r^2}{4\pi^2 G \Sigma^2} \right) + \frac{P_\mathrm{e}}{a^2}, \tag{7}$$

to the lowest order in (H/r). The two terms in the brackets represent, respectively, the gravitational compression and magnetic squeezing of the disk material. The magnetic squeezing term becomes important late in the cloud evolution, when the magnetic field configuration becomes highly pinched. The quantity P_e denotes the ambient pressure that helps confine the disk, especially in low column density regions where gravitational compression is relatively weak.

2.2. Initial Conditions

The "initial" distributions of mass and magnetic flux of a star-forming cloud are not well determined either observationally or theoretically. For illustrative purposes, we prescribe them in a "reference" state, following Basu & Mouschovias (1994). We adopt a uniform distribution

$$B_z^{\mathrm{ref}}(r) = B_\infty, \tag{8}$$

everywhere for the magnetic field, with B_∞ denoting the background field strength, and a simple prescription

$$\Sigma^{\mathrm{ref}}(r) = \frac{\Sigma_0}{\left[1 + (r/r_0)^n\right]^{4/n}}, \tag{9}$$

for the column density, with Σ_0 denoting the central value and r_0 a characteristic radius beyond which the column density drops off rapidly. We will sometimes refer to Σ_0 simply as "the reference column density" later. The prescriptions (8) and (9) are similar to those used by Basu & Mouschovias (1994), except that we leave the exponent n free to specify. The exponent n controls the amount of mass in the central "plateau" region where the mass distribution is more or less uniform. It will play a crucial role in ring formation (§ 3).

The low-column density "envelope" outside the radius r_0 is designed mainly to minimize the effects of cloud boundary on the evolution of the central region. For the model clouds to be considered in the next section, we will adopt a single cloud radius that is twice the characteristic radius r_0. The column density at the cloud edge will then be less than 1/16 of the central value in all cases. A region with such a low column density will be firmly controlled by magnetic fields and its evolution will be effectively decoupled from that of the central region, where dynamic collapse and star formation occur.

The reference model clouds prescribed by equations (8) and (9) are not necessarily in mechanical equilibrium, since the thermal and magnetic forces are not designed to balance out the self-gravity exactly. We let these clouds adjust towards an equilibrium configuration under the constraints (a) that the magnetic field be frozen in matter, and (b) that the field strength remain fixed at the cloud edge (so that continuity with the background field is preserved, see Basu & Mouschovias 1994). The first constraint guarantees that mass-to-flux ratio is conserved for each individual mass element during the adjustment. The second constraint, together with the first, implies that the column density at the cloud edge remains fixed as well. Numerically, the equilibrium configurations are obtained by evolving the reference clouds in time according to the governing equations (1)-(3), setting the velocity of magnetic field lines $V_{_B}$ equal to the velocity V of neutral matter. An extra damping force proportional to $-V$ is applied to the right hand side of the momentum equation (2) during this adjustment phase to gradually bring the reference clouds into a static equilibrium. The final equilibrium configurations, in which $V = 0$ and the self-gravity is balanced exactly by a combination of thermal and magnetic forces, serve as the initial configurations for the subsequent cloud evolution driven by ambipolar diffusion. For the magnetically sub-critical clouds that we are interested in, the adjustment is usually rather small, as noted previously by Basu & Mouschovias (1994).

2.3. Dimensional Units and Dimensionless Quantities

The governing equations (1)-(3) are to be solved numerically. To facilitate the numerical attack, we first cast all dimensional quantities in these equations into a dimensionless form. We begin by normalizing the column density and radius with the central value Σ_0 and characteristic radius r_0 that appear in the reference column density distribution, equation (9), and denote the resultant dimensionless quantities by

$$\sigma \equiv \frac{\Sigma}{\Sigma_0}; \qquad \xi \equiv \frac{r}{r_0}. \tag{10}$$

For typical values of Σ_0 and r_0, we adopt 10^{-2} g cm^{-2} (corresponding to a molecular hydrogen number column density of 2.1×10^{21}cm^{-2}, or roughly two magnitudes of mean visual extinction, e.g., McKee 1989) and 1 pc. These typical values introduce two scaling factors $\mu_\Sigma \equiv \Sigma_0/(10^{-2}$ g cm$^{-2})$ and $\mu_r \equiv r_0/(1$ pc). The dimensional units for other quantities are then obtained from various combinations of Σ_0 and r_0. In terms of the scaling factors μ_Σ and μ_r, we have the following: $M_0 = 2\pi\Sigma_0 r_0^2 = 3.0 \times 10^2(\mu_\Sigma\mu_r^2)$ M$_\odot$ for mass, $V_0 = (GM_0/r_0)^{1/2} = 1.1\ (\mu_r\mu_\Sigma)^{1/2}$ km s^{-1} for velocity, $t_0 = r_0/V_0 = 8.6 \times 10^5(\mu_r/\mu_\Sigma)^{1/2}$ years for time, $B_\infty = \Gamma(2\pi G^{1/2}\Sigma_0) = 16\ \Gamma\ \mu_\Sigma$ μG for field strength, $\rho_0 = \Sigma_0/r_0 = 3.2 \times 10^{-21}(\mu_\Sigma/\mu_r)$ g cm^{-3} for mass density, and $P_0 = \pi G\Sigma_0^2/2 = 1.0 \times 10^{-11}\mu_\Sigma^2$ dyn cm^{-2} for pressure. Note that the dimensionless parameter Γ is the ratio of the background field strength to the critical field strength, $2\pi G^{1/2}\Sigma_0$, associated with the reference column density Σ_0. It is a free parameter that characterizes the degree of cloud magnetization. Note also that the units t_0 and V_0 are the characteristic free fall time and free fall speed of the reference cloud.

With the above defined units, we obtain the following dimensionless quantities

$$m \equiv \frac{M}{M_0};\quad h \equiv \frac{H}{r_0};\quad b_r \equiv \frac{B_r}{B_\infty};\quad b_z \equiv \frac{B_z}{B_\infty};\quad \tau \equiv \frac{t}{t_0};$$

$$v \equiv \frac{V}{V_0};\quad v_{_B} \equiv \frac{V_B}{V_0};\quad \hat{a} \equiv \frac{a}{V_0};\quad \hat{g}_r \equiv \frac{g_r}{V_0^2/r_0};\quad \hat{\rho} \equiv \frac{\rho}{\rho_0};\quad p_{\rm e} \equiv \frac{P_{\rm e}}{P_0}. \tag{11}$$

The dimensionless effective sound speed $\hat{a}$, which will play an important role in ring formation (§3), can be written in terms of the effective cloud temperature $T_{\rm eff}$ as

$$\hat{a} = 0.29\ \left(\frac{1}{\mu_r\mu_\Sigma}\right)^{1/2}\left(\frac{T_{\rm eff}}{30\ {\rm K}}\right)^{1/2}, \tag{12}$$

where a helium abundance of 10% by number has been assumed. Combining equations (7) and (12), we find a molecular hydrogen number density of

$$n_{_{\rm H_2}}^{\rm ref} = 2.2 \times 10^3\ (1 + p_e)\ \mu_\Sigma^2\left(\frac{30\ {\rm K}}{T_{\rm eff}}\right)\ \ {\rm cm}^{-3}, \tag{13}$$

at the center of the reference clouds, where $\Sigma = \Sigma_0$ and $B_r = 0$ (by symmetry). In the fiducial case of $\mu_\Sigma = 1$, $T_{\rm eff} = 30$ K and $p_e \ll 1$ (i.e., gravity dominating external pressure in compressing the cloud center), the above number density is typical of the ^{13}CO clumps found in many molecular clouds. The clumps are often taken as the starting point of isolated star formation calculations. For cluster forming regions, somewhat higher reference density and effective temperature may be more appropriate.

2.4. Dimensionless Governing Equations and Boundary Conditions

We rewrite the governing equations of cloud evolution into a dimensionless, *Lagrangian* form using the dimensionless time τ and mass m as independent variables:

$$\frac{\partial \xi}{\partial m} = \frac{1}{\sigma \xi}, \tag{14}$$

$$\frac{\partial \xi}{\partial \tau} = v, \tag{15}$$

$$\frac{\partial v}{\partial \tau} = \hat{g}_r + \frac{\Gamma^2 b_r b_z}{\sigma} - \hat{a}^2 \xi \frac{\partial \sigma}{\partial m} - \Gamma^2 h \xi \frac{\partial}{\partial m}\left(\frac{b_z^2}{2}\right), \tag{16}$$

$$\frac{\partial}{\partial \tau}\left(\frac{b_z}{\sigma}\right) = -\frac{\partial}{\partial m}[\xi b_z (v_{_B} - v)]. \tag{17}$$

The dimensionless drift velocity between magnetic field lines and neutral cloud matter that appears in the field diffusion equation (17) is given by

$$v_{_B} - v = \frac{\Gamma^2}{\nu_c \hat{\rho}^{1/2}}\left[\frac{b_r b_z}{\sigma} - h\xi \frac{\partial}{\partial m}\left(\frac{b_z^2}{2}\right)\right], \tag{18}$$

where the magnetic coupling coefficient ν_c has a value of 11.6 for the simplest case of coupling given by equation (5). The dimensionless half thickness and mass density of the disk are determined from

$$h = \frac{2\hat{a}^2}{\sigma}\left(1 + \frac{\Gamma^2 b_r^2 + p_{\rm e}}{\sigma^2}\right)^{-1}, \tag{19}$$

and

$$\hat{\rho} = \frac{\sigma^2}{4\hat{a}^2}\left(1 + \frac{\Gamma^2 b_r^2 + p_{\rm e}}{\sigma^2}\right). \tag{20}$$

Together with the auxiliary equations (18)-(20), the four governing equations (14)-(17) completely determine the time evolution of four cloud quantities: column density σ, radius ξ, radial velocity v and the vertical field strength b_z, provided that the radial component of gravity $\hat{g}_r$ and the radial field strength b_r are determined. These two quantities are determined approximately as follows.

It is well known that the radial component of gravity on an infinitely thin disk with column density $\sigma(\xi)$ is given by

$$\hat{g}_r = \int_0^\infty \xi' \sigma(\xi') M(\xi, \xi')\, d\xi', \tag{21}$$

where the integral kernel is obtained from

$$M(\xi, \xi') = \left(\frac{2}{\pi}\right)\frac{d}{d\xi}\left[\frac{1}{\xi_{\rm max}} K\left(\frac{\xi_{\rm min}}{\xi_{\rm max}}\right)\right], \tag{22}$$

with $\xi_{\rm min}$ =min(ξ, ξ'), $\xi_{\rm max}$ =max(ξ, ξ') and K being the complete elliptic integral of the first kind. Following Ciolek & Mouschovias (1993), we shall use equation (21) to approximate the radial component of gravity for our thin disk of finite thickness.

On an infinitely thin disk, the radial field strength b_r can be determined from the vertical field strength b_z. We adopt the formalism of Lubow, Papaloizou & Pringle (1993), who assumed that the magnetic field consists of two parts: a uniform background and a potential field due to a toroidal current confined entirely to the disk. The first part is prescribed, and the second part is determined solely by the (vertically-integrated) toroidal current density J_ϕ, which is linearly proportional to b_r on the disk. In particular, b_z on the disk can be expressed as an integral over disk radius with an integrand that is linearly proportional to J_ϕ (Jackson 1975), and thus b_r. A simple matrix inversion then allows one to calculate b_r in terms of b_z (see Lubow et al. 1993 for details). As an approximation, we shall use the above formalism to compute the radial field strength for our thin disk of finite thickness.

For boundary conditions, we impose at the center of the cloud (where $m = 0$) the conditions of symmetry: $\xi = 0$, $v = 0$, $\partial b_z/\partial m = 0$, and $\partial\sigma/\partial m = 0$. At the outer edge, we let the cloud boundary move freely while holding the vertical component of magnetic field b_z and the column density of the disk σ fixed at their initial values at all times, consistent with the boundary conditions we imposed in § 2.2 during the adjustment from the reference state towards the equilibrium configuration. These specifications complete our discussion of governing equations, initial and boundary conditions.

2.5. Numerical Method

The numerical methods for Lagrangian hydrodynamics and magnetohydrodynamics are well documented in Chapters 4 and 8 of Bowers & Wilson (1991), respectively. We follow the procedures outlined in those chapters closely, except for the treatment of magnetic field diffusion equation (17). The field diffusion is driven by a combination of magnetic tension and pressure forces, corresponding to the two terms on the right hand side of equation (18). We use the method of operator splitting to treat the two driving terms separately. While the usual finite differencing is adequate for the tension term, special treatment is necessary for the magnetic pressure term to ensure stability; for the pressure term, we employ the so-called "Gaussian elimination" technique, as described in section 6.4 of Bowers & Wilson (1991).

3. RING FORMATION IN MAGNETICALLY SUBCRITICAL CLOUDS

In this section, we numerically integrate the non-dimensional governing equations (14)-(17), subject to the initial and boundary conditions described in § 2.2 and § 2.4. Two dimensionless constants appear in the governing equations: Γ, the ratio of the background field strength B_∞ to the critical field strength $2\pi G^{1/2}\Sigma_0$, and $\hat{a}$, the dimensionless effective sound speed. The quantity Γ controls the degree of cloud magnetization, and must be greater than unity in order for the clouds to be mainly supported by (ordered) magnetic fields. Although Nakano (1998) presented theoretical arguments against star-forming clumps being magnetically subcritical, the situation is less clear observationally: Zeeman measurements of the field strength in molecular clouds, as compiled by Crutcher (1999), is roughly consistent with the clouds being magnetically critical, after likely geometric corrections (Shu et al. 1999). Uncertainties involved in estimating the mass-to-flux ratio preclude a firmer conclusion. We believe that at least some star-forming clumps are magnetically subcritical *to begin with*[1], and adopt for definitiveness a round value of $\Gamma = 2$. Clouds with values of Γ substantially less than 2 will not be disk-like and the thin-disk approximation adopted here may not be applicable. Values of Γ much larger than 2, on the other hand, are difficult to reconcile with the Zeeman measurements. For the dimensionless effective sound speed, we will first adopt a round value of $\hat{a} = 0.3$ (corresponding to an effective temperature of 32 K for the canonical choice of the scaling factors $\mu_r = \mu_\Sigma = 1$), and then consider a smaller value of $\hat{a} = 0.2$ for comparison. A third constant, the dimensionless external pressure $p_{\rm e}$, appears in auxiliary equations (19) and (20). We adopt, for simplicity, a value of $p_{\rm e} = 0.1$, which corresponds to a reasonable dimensional value of $10^{-12}\mu_\Sigma^2$ dyn cm^{-2}.

Three model clouds are considered. They have, respectively, $n = 2$, 4 and 8, where n is the exponent that specifies the column density distribution in the reference state. A quick inspection of the prescription of the reference column density distribution, equation (9), reveals that the $n = 8$ cloud has the largest cloud mass for the same cloud radius (taken to be twice the characteristic radius r_0 for all clouds, as mentioned earlier). Its dimensionless mass is 0.80, compared with 0.40 (0.66) for the $n = 2$ (4) cloud. The Jeans mass is, on the other hand, much smaller, at least near the cloud center, where

$$M_J = \frac{1.17 a^4}{G^2 \Sigma_0}, \tag{23}$$

according to Larson (1985; his equation [9]). The dimensionless central Jeans mass takes

[1]We note that some Zeeman measurements are for *evolved* regions where the mass-to-flux ratio may have already been increased through ambipolar diffusion to supercritical values (McKee 1999).

the following simple form

$$m_J = 7.35\hat{a}^4, \tag{24}$$

which has a value of 0.06 for our standard choice of dimensionless sound speed $\hat{a} = 0.3$.

The reference clouds are allowed to settle towards an equilibrium configuration under the influence of an artificial damping force, with magnetic flux frozen-in, as described in §2.2. After the equilibrium state is reached, we reset the time t to zero and turn on ambipolar diffusion. The clouds then evolve on the magnetic flux redistribution time scale, which is typically an order of magnitude longer than the dynamic time scale. In what follows, we will illustrate the main features of cloud evolution by displaying various cloud quantities at the initial equilibrium time $t = 0$ and two representative times, t_1 and t_2, when the maximum column density reaches, respectively, 10 and 10^2 times the reference value Σ_0. Typically, by the time t_1, the clouds start to become magnetically supercritical, and are about to collapse dynamically. By the time t_2, the collapse is well into the dynamic phase, with a maximum infall speed comparable to, or greater than, the effective sound speed a.

First, we plot the distributions of column density and infall velocity at the time $t = 0$ and t_1 in Fig. 1. The latter time corresponds to 6.75, 7.87, and 8.63 million years [2] for the $n = 2$, 4, and 8 cloud, respectively. The column density distributions at time t_1 illustrate clearly two distinctive modes of cloud evolution: in the $n = 2$ cloud with a relatively peaky initial mass distribution (see the insert), a dense core has formed at the center. The more massive $n = 8$ cloud with a flatter central mass distribution has produced, on the other hand, a dense ring. The intermediate $n = 4$ cloud is close to the borderline between core-forming and ring-forming; a slight increase of the exponent n, to a value of 4.2 for example, would induce the cloud to form a ring instead of a core.

Both the central cores and dense ring are formed quasi-statically, as indicated by the velocity distributions shown in panel (b) of Fig. 1. Although the maximum infall speeds are substantial, ranging from ~ 0.05 to ~ 0.22 km s^{-1} in our particular examples, they remain below the effective sound speed (and should be even smaller compared with the magneto-sonic speed, the relevant signal speed in a magnetized cloud). Note that the (subsonic) infall regions are clearly "large scale", spanning a good fraction of a parsec, even during this relatively early "starless" phase of evolution (see also Li 1999 and Ciolek & Basu 2000). Such an extended infall motion may have been detected in the starless core L1544 (Taffala et al. 1998; Williams et al. 1999). For starless cores formed in magnetically

[2]We set the scaling factor μ_r and μ_Σ to unity hereafter (including in the figures) to obtain concrete dimensional quantities from the dimensionless numerical solutions. The dependences of dimensional units on μ_r and μ_Σ are given in §2.3.

subcritical clouds, Ciolek & Basu (2000) showed that the infall speed is sensitive to the background field strength (i.e., the value of Γ in our notation). Panel (b) demonstrates that the speed depends rather strongly on the initial mass distribution as well.

Second, we plot, in Fig. 2, the distributions of mass-to-flux ratio and the cloud shapes at the time $t = 0$ and t_2. The latter time corresponds to 6.95, 8.10, and 8.94 million years for the $n = 2$, 4, and 8 cloud, respectively. By the time t_2, a substantial amount of mass (14, 55, and 90 $M_\odot$, respectively) has become magnetically supercritical, inside either the central core or dense ring, according to panel (a). Note that the mass-to-flux ratio of the $n = 8$ cloud peaks inside the ring, and that the central region interior to the ring remains magnetically subcritical. The relatively strong central field should cushion the contraction of the ring towards the origin as a whole, with potentially observable signatures.

The cloud shapes, as outlined by the half thickness H defined in equation (6) and shown in panels (b)-(d) of Fig. 2, change dramatically as the clouds evolve. The minimum thickness occurs at the column density maximum inside either the central cores or dense ring, where self-gravity squeezes on the disk material the hardest. The lower-column density "envelope" is compressed, in contrast, mainly by external pressure. Together, the self-gravity and external pressure keep the cloud material flattened at all times, justifying the thin-disk approximation adopted. Also shown in panels (b)-(d) are magnetic field lines at time t_2. It is clear that mass accumulation in the core ($n = 2$ and 4) and the ring ($n = 8$) has also led to an accumulation of magnetic flux in these over dense regions, creating a pinched magnetic configuration. Indeed, the mass-to-flux ratio at time t_2 remains less than twice the critical value everywhere (see panel [a]), even though the column density has increased by a factor of nearly 10^2 from its initial value, and the volume density by an even larger factor, close to 10^4. The near critical mass-to-flux ratio and associated strong magnetic field are characteristic of dense cores (see, e.g., Lizano & Shu 1989 and Basu & Mouschovias 1994) and rings formed out of magnetically subcritical clouds, in contrast with those formed in other (weakly- or non-magnetic) scenarios.

The dichotomy of core and ring formation is illustrated most vividly by Fig. 3, where the column density distributions of the core-forming $n = 2$ and ring-forming $n = 8$ cloud are represented graphically at the time $t = 0$, t_1 and t_2. The dense, opaque central core of the $n = 2$ cloud is expected to collapse quickly, on a (very short, local) dynamic time scale, to produce a single, isolated star. What happens to the ring? In §4.1 below, we will argue that the dense, self-gravitating ring is likely to fragment into smaller pieces, which collapse to form more than one star. Therefore, the dichotomy of core and ring formation should be indicative of two modes of star formation in a strongly magnetized cloud: a single, isolated mode and a multiple, clustered mode, depending on the mass of the cloud and its

distribution.

So far, we have concentrated on how mass distribution, as specified by the exponent n in equation (9), affects core and ring formation. We now wish to demonstrate that the effective sound speed, a, has a profound effect as well. For this purpose, we repeat the evolution of the same three clouds shown in Figs. 1-3 with a smaller value of dimensionless sound speed $\hat{a} = 0.2$ (instead of 0.3). We find that, whereas the $n = 2$ ($n = 8$) cloud forms a central core (dense ring) as before, the borderline $n = 4$ cloud is induced by the lower sound speed to collapse off-center into a ring instead of a central core. This difference is consistent with the trend found by Bastien (1983) for flattened, *non-magnetic* clouds: decreasing the sound speed (and thus the Jeans mass) makes ring formation easier. Indeed, if we were to remove all of the magnetic fields from our magnetically supported clouds suddenly (assuming $\hat{a} = 0.2$), they would collapse promptly, with the $n = 2$ cloud forming a dense core and the $n = 4$ and 8 cloud each forming a dense ring, just as their magnetized counterparts. The strong magnetic fields lengthen the ring formation time (by roughly an order of magnitude), but do not appear to suppress the ring formation tendency of a multi-Jeans mass cloud with a relatively flat mass distribution. Indeed, it is the magnetic fields that are responsible for the cloud flattening and thus the ring formation in the first place. We have explored other forms of mass and magnetic flux distribution as well as other values of the dimensionless sound speed $\hat{a}$, and come to the same general conclusion.

Finally, we note that Mouschovias and collaborators have studied the ambipolar diffusion-driven evolution of disk-like magnetic clouds extensively (e.g., Ciolek & Mouschovias 1994; Basu & Mouschovias 1994, 1995), although none of their models produced a dense ring. The lack of ring formation in their models can be traced to the particular form of reference mass distribution adopted, which is similar to the relatively peaky distribution of the core-forming $n = 2$ cloud shown in Figs. 1-3 (cf. equation [31] of Basu & Mouschovias 1994). Our more flexible prescription of mass distribution enables us to uncover a new outcome to the ambipolar diffusion-driven evolution of magnetically subcritical clouds - ring formation, which has implications on cloud fragmentation and multiple star formation.

4. DISCUSSION AND IMPLICATIONS

4.1. Ring Fragmentation

Dense, self-gravitating rings like the one shown in the right column of Fig. 3 contain many Jeans masses, and are thus susceptible to breaking up gravitationally into a number

of smaller pieces. The fact that they are gradually condensed out of strongly magnetized clouds modifies their fragmentation properties in two important ways.

First, the strong magnetic fields present during the initial *magnetically subcritical*, quasi-static phase of cloud evolution prevents the Jeans instability from developing on a dynamic time scale everywhere, including inside the forming rings (Langer 1978; Nakano 1988). On the other hand, after becoming substantially *supercritical*, the dense rings collapse dynamically, leaving little time for small fragments to grow. It therefore appears that the best time for the rings to break up gravitationally is during the transitional period when they are marginally magnetically critical, after being freed from the firm grips of magnetic fields through ambipolar diffusion, but before embarking on a runaway collapse. If this is indeed the case, then we can estimate the number of fragments expected from the breakup. For typical dark cloud conditions, the transition occurs roughly around the time t_1, when the maximum column density reaches 10 times the reference value Σ_0. Since the ring is narrow and self-gravitating at this time, it should fragment in a way similar to that of an infinitely long self-gravitating cylinder. It is well known (Larson 1985) that (non-magnetic) cylinders with a sound speed a and central mass density $\rho_{\rm c}$ are unstable to perturbations with wavelength exceeding about

$$\lambda_{\rm cr} = 4 \left(\frac{2a^2}{\pi G \rho_{\rm c}} \right)^{1/2}. \tag{25}$$

The instability grows fastest at a wavelength near $2\lambda_{\rm cr}$ (Inutsuka & Miyama 1992). For a ring centered at $r_{\rm r}$, one expects the number of fragments to be roughly

$$N \approx \frac{2\pi r_{\rm r}}{2\lambda_{\rm cr}} \approx \frac{\pi \sigma_{\rm r} \xi_{\rm r}}{16 \hat{a}^2}, \tag{26}$$

where $\sigma_{\rm r}$ and $\xi_{\rm r}$ are the dimensionless column density and radius at the ring location. We have used equations (7) and (25) in deriving the second expression, also taking into account the fact that the ring is mainly compressed by self-gravity. Applying the above formula to the marginally critical ring shown in the middle right panel of Fig. 3, we find the expected number of fragments to be ~ 5 (with $\sigma_{\rm r} = 10$, $\xi_{\rm r} = 0.23$, and $\hat{a} = 0.3$). If the dimensionless effective sound speed $\hat{a}$ is lowered to 0.2, then the same cloud would produce ~ 19 fragments instead (with $\sigma_{\rm r} = 10$ and $\xi_{\rm r} = 0.38$). Clearly, the number of fragments increases quickly with decreasing sound speed, as one might expect intuitively.

The second modification introduced by a strong magnetic field is the possibility of interchange instability. In the simplest case of an infinitely thin disk supported entirely (and statically) by a magnetic field, the square of the growth rate γ is given by (see Spruit & Taam 1990)

$$\gamma^2 = -\frac{d[\ln(\Sigma/B_z)]}{dr} \cdot g_r, \tag{27}$$

where g_r denotes the radial component of gravity as before. The above equation implies that this (local) instability will grow (i.e., $\gamma^2 > 0$) as long as the mass-to-flux ratio, Σ/B_z, decreases in the direction of gravity, g_r. This criterion will be satisfied in part of the ring during its (long) quasi-static phase of formation. The reason is simply that the mass-to-flux ratio peaks inside the ring (see Fig. 2a), and thus decreases towards the origin, which is also the direction of gravity during most of the quasi-static phase of cloud evolution. The instability is demonstrated explicitly in Fig. 4, where γ^2 is plotted against the radius and mass for the ring-forming $n = 8$ cloud shown in Figs. 1-3 at four relatively early times: the initial equilibrium time $t = 0$ and the three times when the maximum column density reaches 2, 4, and 8 times the reference value Σ_0 (corresponding to 5.39, 7.76, and 8.52 million years), respectively. Note that the inner, plateau part of the cloud (where star formation occurs) starts out close to being marginally stable. It becomes increasingly more unstable as the ring condenses out, until enough mass has accumulated in the ring to reverse the direction of the gravity interior to the ring (to outward-pointing). The reversal explains the suppression of instability near the center at the last time shown. It is likely that magnetic interchange instability, which is intrinsic to the ring formation process, contributes significantly to ring fragmentation, once the axisymmetry is removed. The situation may be complicated, however, by ambipolar diffusion and the associated drift between magnetic field lines and cloud matter. Non-axisymmetric models are required to examine the interplay between magnetic interchange instability and cloud fragmentation in detail.

4.2. A Scenario of Multiple Star Formation

Multi-Jeans mass clouds are unstable to forming multiple fragments of Jeans mass. The presence of a strong magnetic field in a lightly ionized medium such as molecular cloud does not change the minimum wavelength (and thus mass) for instability, although the growth time could be greatly lengthened, according to the linear analysis of Langer (1978). We have shown that nonlinear developments of this magnetically-retarded Jeans instability lead, in a strict axisymmetric geometry, to the formation of dense, self-gravitating rings that are prone to breaking up into smaller pieces. Generalizing the ring formation and fragmentation to non-axisymmetric clouds, we propose the following scenario for multiple star formation. As magnetically subcritical, multi-Jeans mass clouds evolve due to ambipolar diffusion, dense elongated substructures develop quasi-statically. These substructures break up, through Jeans and possibly magnetic interchange instabilities, into a number of smaller pieces, creating a cluster of dense, magnetically supercritical cores. The supercritical cores collapse quickly in a (local) dynamic time, leading to a burst of star formation.

The above scenario is a direct extension of the standard picture of isolated star formation (Shu et al. 1987; Mouschovias & Ciolek 1999) to the formation of multiple stars. A key ingredient is the gradual condensation of elongated multi-Jeans mass substructures capable of breaking up into multiple dense cores. If the breakup occurs mostly during the transitional period when the substructure is approximately magnetically critical, as we speculated in the last subsection, then the initial size of the dense cores and the separation between neighboring cores would be comparable to the Jeans length scale evaluated at the magnetically critical density (cf. equation [25]). The same size scale applies to supercritical dense cores formed in isolation, as pointed out by Basu & Mouschovias (1995).

Although details remain to be worked out, we anticipate two potentially observable features of the multiple cores formed in the above scenario. First, as with single cores formed through ambipolar diffusion in isolated star formation (e.g., Lizano & Shu 1989; Basu & Mouschovias 1994), the multiple cores should have magnetic field strength close to (say, within a factor of two of) the critical value, even after they become supercritical and after star formation. Second, the cores should have small motions relative to one another, since the motions are cushioned by both the magnetic flux trapped inside the cores and the flux held in between them (see Fig. 2d). These features are not expected from cores formed, e.g., in prompt collapse of non-magnetic Jeans-unstable clouds (Klessen et al. 1998). Observations of mass-to-flux ratio and relative motions of dense cores can provide key tests of various scenarios of multiple star formation.

To make the scenario more quantitative, one needs to construct non-axisymmetric models. Such models will allow one to follow the ring fragmentation process and, more importantly, to study the formation and fragmentation of over dense substructures in more realistic clouds that are irregular in shape and/or contain appreciable substructures in mass distribution to begin with. Moreover, once formed, the fragments (i.e., multiple cores) are expected to interact with one another and with their common envelope, both gravitationally and magnetically. The interaction should play a role in determining the mass spectrum and motions of the cores and thus stars (Motte, Andre & Neri 1998; Testi & Sargent 1998). In particular, gravitational drag effect analogous to the "dynamic friction" in stellar dynamics could in principle bring the cores closer together to form binaries and multiple stellar systems (Larson 2000). Non-axisymmetric models will also be required to follow the nonlinear developments of the (dynamic) Jeans and magnetic interchange instabilities, which could provide an important source of turbulence (see also Zweibel 1998). They may explain, at least in part, why cluster forming regions are more turbulent than isolated star forming regions, even before stars are formed.

We should stress that the above scenario is intended mainly for the formation of stellar

groups and small clusters in relatively quiescent regions of molecular clouds, such as the fragmented starless cores observed in millimeter continuum by Ward-Thompson, Motte & Andre (1999), and perhaps the ρ Oph B2 core studied in detail by Motte et al. (1998). The ρ Oph B2 core has apparently broken up into a dozen or so starless clumps. It may represent a short-lived phase during the evolution of an initially magnetically subcritical, multi-Jeans mass cloud in which supercritical cores have already formed through ambipolar diffusion and fragmentation, but yet to collapse into a group of stars. The well-studied starless core L1544 may represent a similar short-lived phase during the formation of an isolated magnetized core leading to single star formation (e.g., Williams et al. 1999; Li 1999; Ciolek & Basu 2000). Our scenario for multiple star formation is not directly applicable to the formation of rich clusters, such as the Trapezium cluster in Orion, where turbulence-induced fragmentation probably plays a dominant role (Klessen et al. 1998; Padoan et al. 2000).

4.3. NW Cluster of the Serpens Molecular Cloud Core

Although one does not expect to find many ring-like structures in real star forming regions, because of the high degree of geometric symmetry required, they are sometimes observed. The most famous example is perhaps the ring of massive stars in the massive cluster forming region W49N (Welsh et al. 1987). A more recent example is the northwestern (NW) cluster of protostars and dense cores in the Serpens molecular cloud core – another active (although less massive) cluster-forming region (e.g., Testi & Sargent 1998; Davis et al. 1999). The cluster has the appearance of a tilted, fragmented ring, and could be resulted from the fragmentation of a dense ring-like structure formed quasi-statically in a strongly magnetized cloud. This interpretation is strengthened by polarization measurements of thermal dust emission, which indicates a large scale magnetic field threading the ring plane more or less perpendicularly (Davis et al. 2000), as expected in our scenario (see Fig. 2d). Moreover, the velocity dispersion among the cores is rather small, on the order of 0.25 km s^{-1} (J. Williams, personal communication), which could result from the magnetic cushion effect mentioned earlier. Infall motions are observed on both large, cluster scale ($\sim$ 0.2 pc) and small, individual core/protostar scale ($\sim$ 0.02 pc; Williams & Myers 2000). In our picture, the large- and small-scale infall motions would be associated, respectively, with the process of ring formation as a whole (similar to that shown in Fig. 1b) and with gravitational contraction onto individual cores/protostars, although substantial contributions from localized turbulence dissipation are also possible (Myers & Lazarian 1998). Our interpretation is complicated, however, by the strong turbulent and outflow motions present in the region.

I thank C. Matzner, F. Motte and J. Williams for helpful correspondence and an anonymous referee for useful comments.

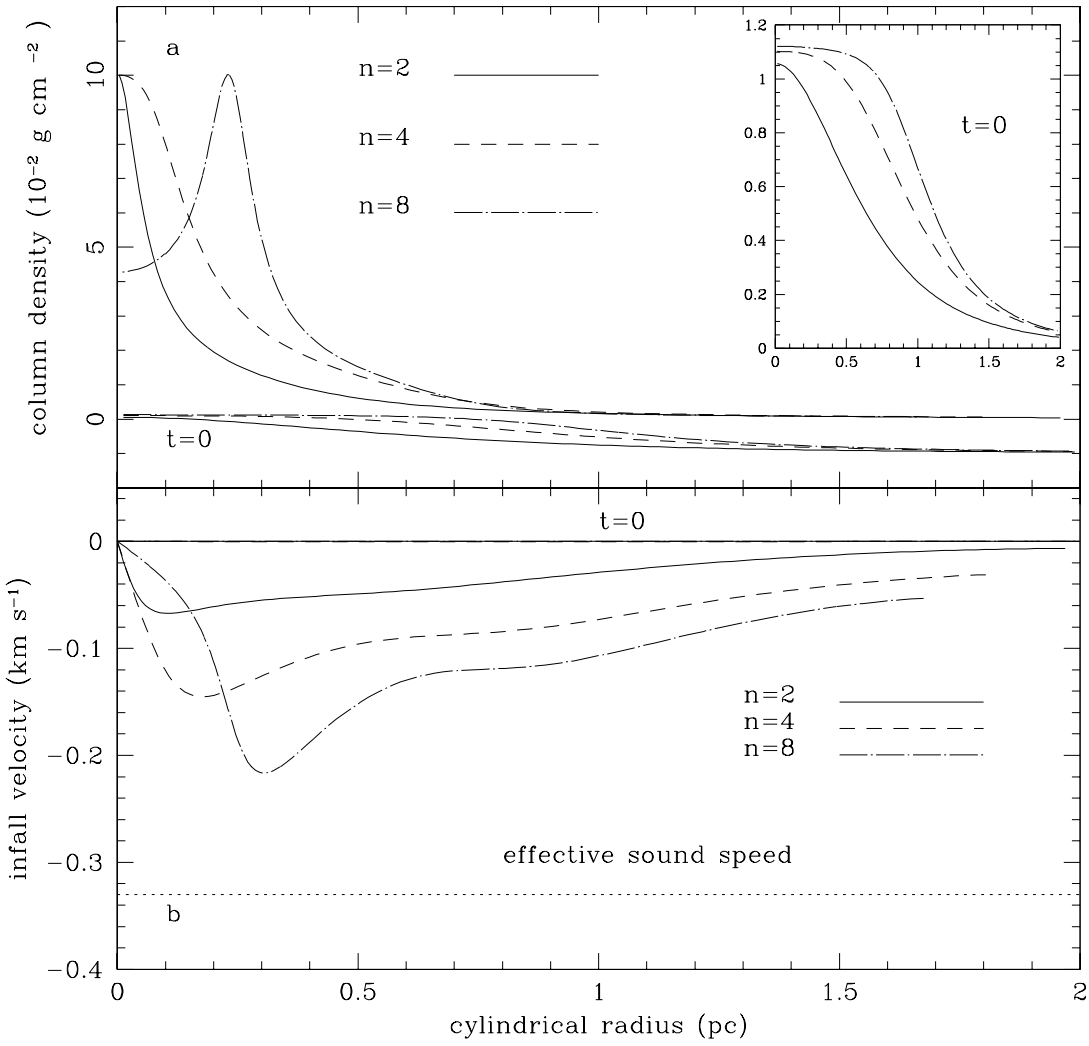

Fig. 1.— Evolution of three magnetized clouds with different initial mass distributions as specified by the exponent n in equation (9). (a) Column density distributions at the initial equilibrium $t = 0$ and the time t_1 when the maximum column density reaches 10 times the reference value Σ_0. Note that a dense core is formed at the center of the $n = 2$ and 4 cloud whereas a dense ring is produced in the $n = 8$ cloud. For clarity, the distributions at $t = 0$ are lowered by one unit. Their differences show up more clearly in the insert. (b) Distributions of infall speed at the same two times as in panel (a), showing the quasi-static nature of ring and core formation, although substantial infall motion is clearly present on the (sub-)parsec scale.

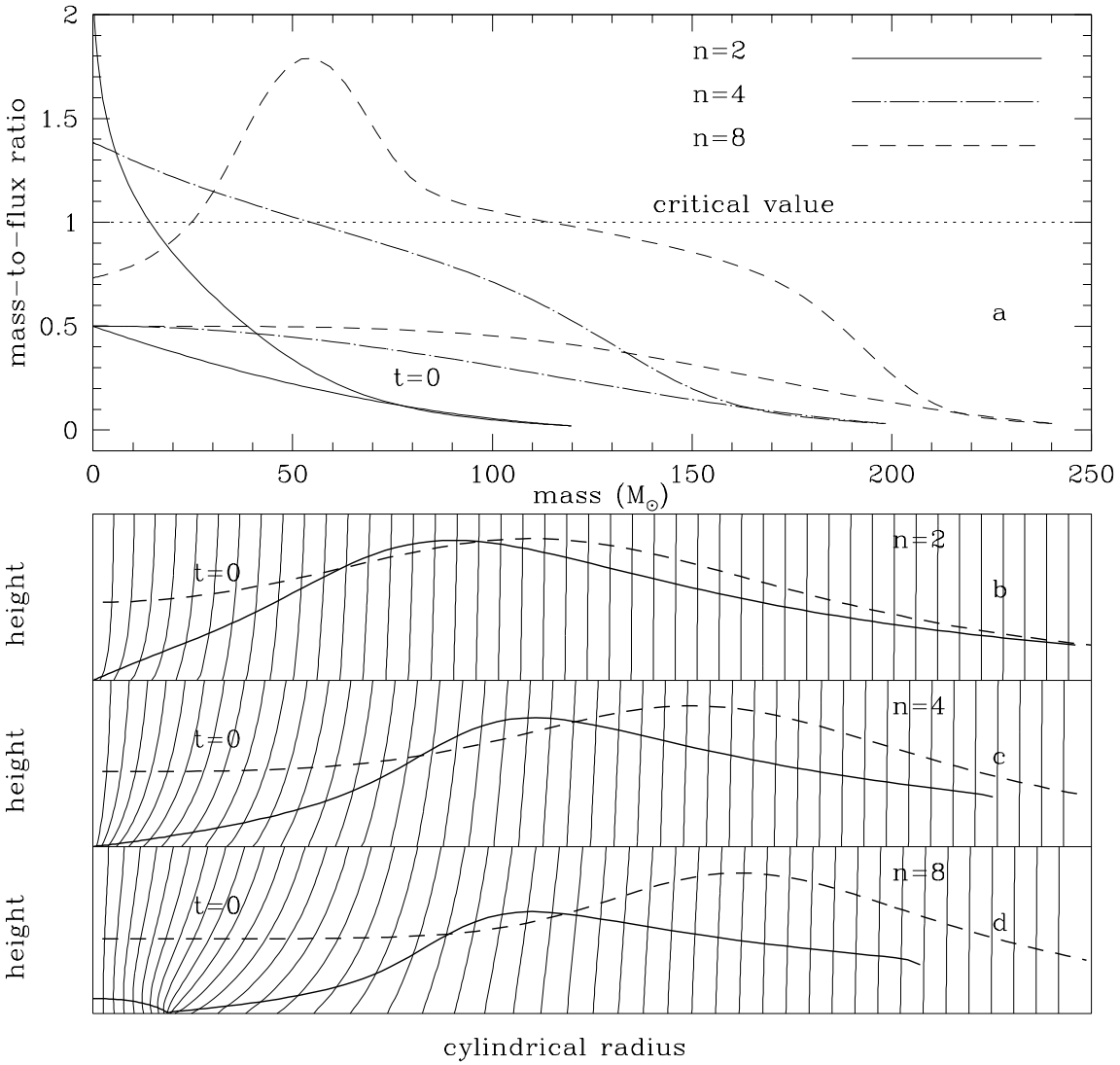

Fig. 2.— Additional properties of the model clouds shown in Fig. 1. (a) Distributions of mass-to-flux ratio, in units of the critical value $(2\pi)^{-1}$ $G^{-1/2}$, as a function of mass at the initial time t=0 and the time t_2 when the maximum column density reaches 10^2 times the reference value Σ_0. Regions above the dotted line are magnetically supercritical. (b)-(d) Magnetic field lines at the time t_2 (thin solid lines) and the disk half thickness at the time t=0 (heavy dashed lines) and the time t_2 (heavy solid lines).

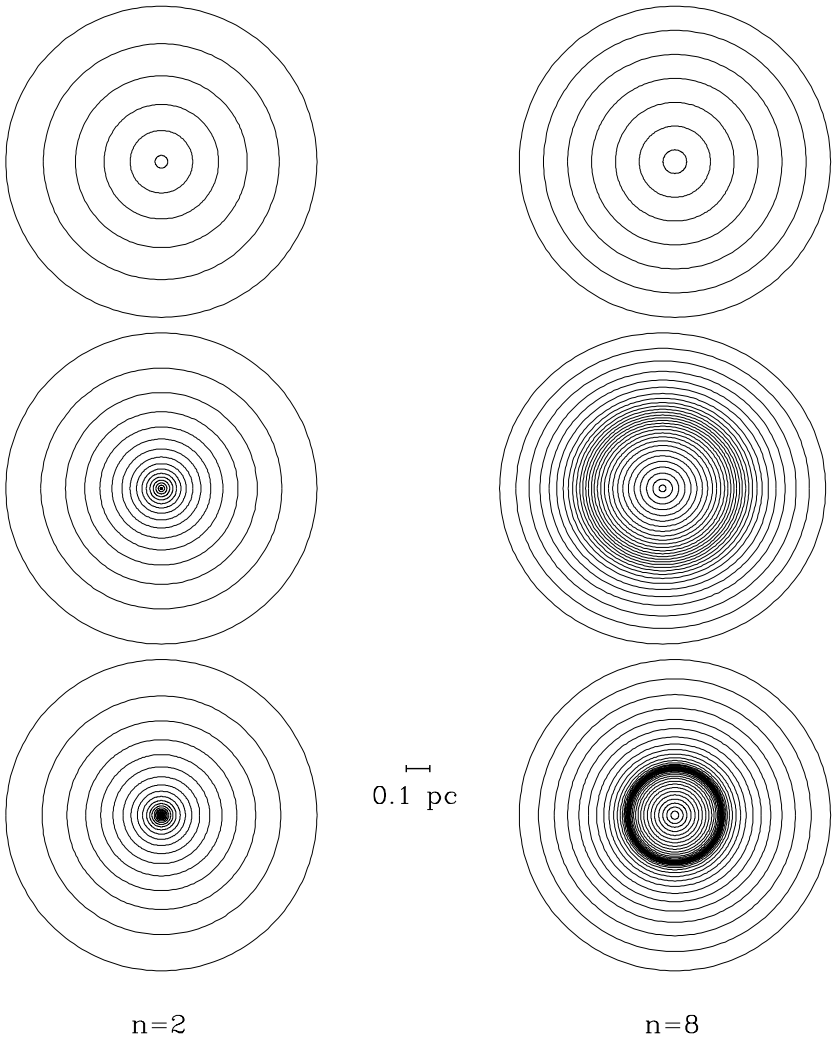

Fig. 3.— Graphical representation of core and ring formation in the inner region (inside a radius of 0.5 pc) of the $n = 2$ (left column) and $n = 8$ (right column) cloud shown in Figs. 1 and 2. Contours are plotted at a separation inversely proportional to the local column density. They are used to visualize the cloud mass distributions at the time $t = 0$ (top), t_1 (middle) and t_2 (bottom), when the maximum visual extinction through the cloud is ~ 2, 20 and 200 magnitudes, respectively.

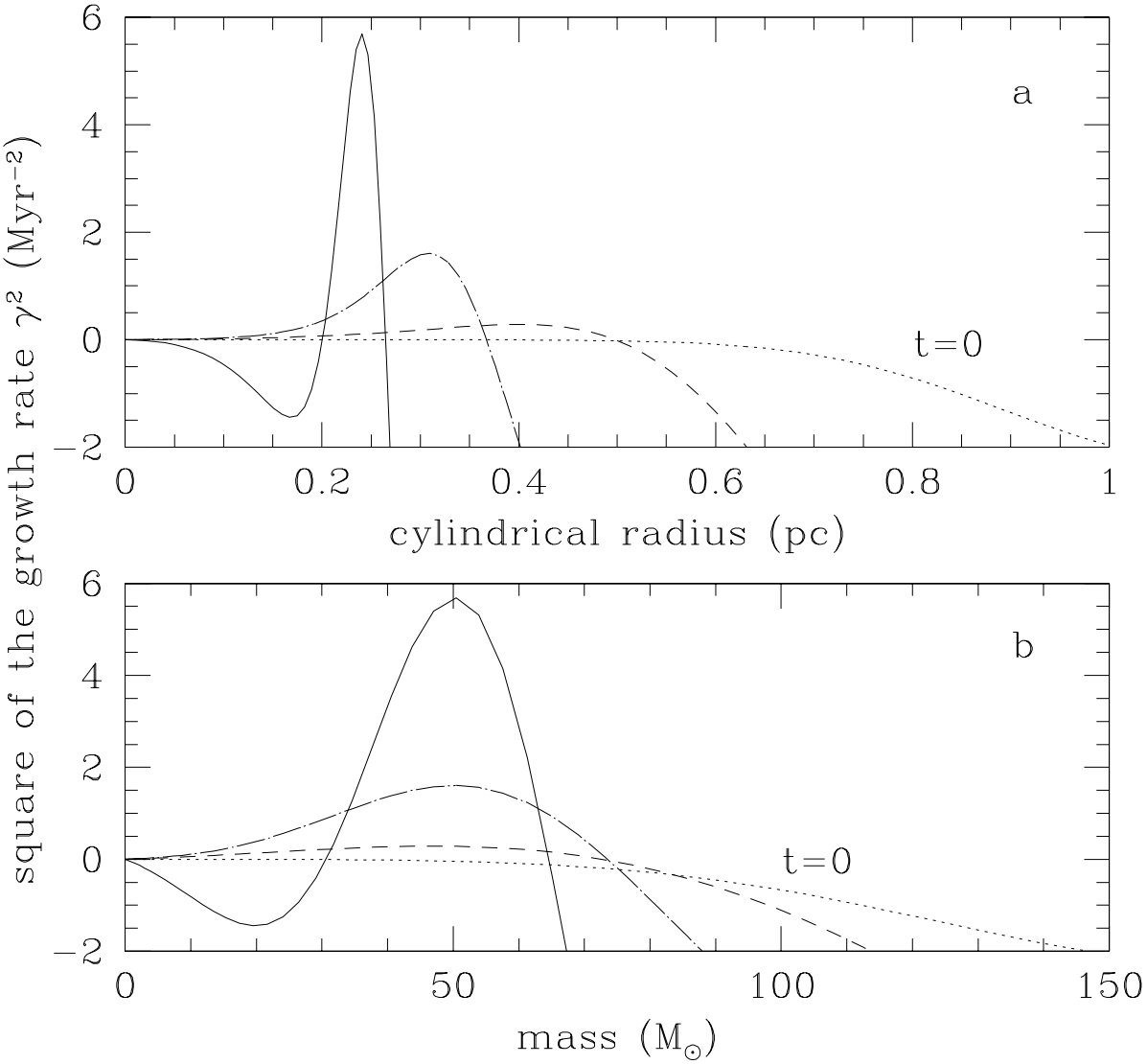

Fig. 4.— The square of the growth rate of magnetic interchange instability, γ^2, in units of the inverse of the square of a million years, plotted against (a) radius and (b) mass of the ring-forming $n = 8$ cloud shown in Fig 3, at the initial equilibrium time $t = 0$ (dotted) and the three times when the maximum column density reaches 2 (dashed), 4 (dash-dotted), and 8 (solid) times the reference value Σ_0, corresponding to 5.39, 7.76, and 8.52 million years. Regions with positive γ^2 are unstable, according to the simple criterion given in the text.

5. REFERENCES

Bastien, P. 1983, AA, 119, 109

Basu, S. & Mouschovias, T. Ch. 1994, ApJ, 432, 720

Beichman, C. A., Myers, P. C., et al. 1986, ApJ, 307, 337

Black, D. C. & Bodenheimer, P. 1976, ApJ, 206, 138

Bonnell, I. A. 1999, in The Origins of Stars and Planetary Systems, eds C. Lada & N. Kylafis (Dordrecht: Kluwer), 479

Boss, A. P. 2001, ApJL, in press

Bowers, P. J. & Wilson, J. R. 1991, Numerical Modeling in Applied Physics and Astrophysics (Boston: Jones and Bartlett Publishers)

Ciolek, G. E. & Basu, S. 2000, ApJ, 529, 925

Ciolek, G. E. & Mouschovias, T. Ch. 1993, ApJ, 418, 774

——, 1994, ApJ, 425, 142

Crutcher, R. M. 1999, ApJ, 520, 706

Davis, C. J., Matthews, H. E., Ray, T. P., Dent, W., Richer, J. S. 1999, MNRAS, 309, 141

Davis, C. J., Chrysostomou, A., Matthews, H. E., Jenness, T., Ray, T. P. 2000, ApJL, in press

Fiedler, R. A. & Mouschovias, T. Ch. 1993, ApJ, 415, 680

Inutsuka, S. & Miyama, S. M. 1992, ApJ, 388, 392

Jackson, J. D. 1975, Classical Electrodynamics (New York: John Wiley & Sons)

Klessen R. S., Burkert, A., & Bate, M. R. 1998, ApJ, 501, L205

Langer, W. D. 1978, ApJ, 225, 95

Larson, R. B., 1985, MNRAS, 214, 379

——, 2000, in The Formation of Binary Stars, eds. R. Mathieu & H. Zinnecker, in press (astro-ph/0006288)

Li, Z.-Y. 1999, ApJ, 526, 806

Lizano, S. & Shu, F. H. 1989, ApJ, 342, 834

Lubow, S. H., Papaloizou, J. C. B., & Pringle, J. E. 1993, MNRAS, 267, 235

McKee, C. F. 1989, ApJ, 345, 782

Motte, F., Andre, P., & Neri, R. 1998, AA, 336, 150

Mouschovias, T. Ch. 1976, ApJ, 206, 753

Mouschovias, T. Ch. & Ciolek, G. E. 1999, in The Origins of Stars and Planetary Systems, eds C. Lada & N. Kylafis (Dordrecht: Kluwer), p305

Mouschovias, T. Ch. & Morton, S. A. 1991, ApJ, 371, 296

Myers, P. C. 1999, in The Origin of Stars and Planet Systems, eds. C. J. Lada & N. D. Kylafis (Kluwer: Dordrecht), p67

Myers, P. C. & Lazarian, A. 1998, ApJ, 507, L157

Nakamura, F., Hanawa, T. & Nakano, T. 1995, ApJ, 444, 770

Nakano, T. 1984, Fundam. Cosmic Phys., 9, 139

——, 1988, PASJ, 40, 593

——, 1998, ApJ, 494, 587

Norman, M. L. & Wilson, J. R. 1978, ApJ, 224, 497

Norman, M. L. & Wilson, J. R., & Barton, R. T. 1980, ApJ, 239, 968

Padoan, P., Nordlund, A., Rognvaldsson, O., Goodman, A. 2000, in From Darkness to Light, eds. T. Montmerle & Ph. Andre (ASP Conference Series), in press

Pudritz, R. E. 1990, ApJ, 350, 195

Shu, F. H. 1992, The Physics of Astrophysics II (Mill Valley: University Science Books)

Shu, F. H., Adams, F. C. & Lizano, S. 1987, ARAA, 25, 23

Shu, F. H., Allen, A., Shang, H., Ostriker, E. & Li, Z.-Y. 1999, in The Origins of Stars and

Planetary Systems, eds. C. Lada & N. Kylafis (Dordrecht: Kluwer), p193

Shu, F. H. & Li, Z.-Y. 1997, ApJ, 475, 251

Spruit, H. C. & Taam, R. E. 1990, AA, 229, 475

Taffala, M., Mardones, D., Myers, P. C., Caselli, P., Bachiller, R., & Benson, P. J. 1998, ApJ, 504, 900

Testi, L. & Sargent, A. I. 1998, ApJ, 508, L91

Tomisaka, K., Ikeuchi, S., & Nakamura, T. 1988, ApJ, 335, 239

Vazquez-Semadeni, E., Ostriker, E. C., Passot, T., Gammie, C. F., & Stone, J. M. 1999, in Protostars and Planets IV, eds. V. Mannings, A. Boss, & S. Russell (Univ. Arizona Press: Tucson), p3

Ward-Thompson, D., Motte, F. & Andre, P. 1999, MNRAS, 305, 143

Welsh, W. J., Jackson, J. M., Dreher, J. W., Terebey, S. & Vogel, S. N. 1987, Science, 238, 1550

Williams, J. P. & Myers, P. C. 2000, ApJ, in press

Williams, J. P., Myers, P. C., Wilner, D. J. & di Francesco, J. 1999, ApJ, 613, L61

Zweibel, E. G. 1998, ApJ, 499, 746